*Research sponsored by the U. S. Atomic Energy Commission under contract with Union Carbide Corporation.

†Guest scientist from Japan Atomic Energy Research Institute, Tokai, Iburaki, Japan.

‡Oak Ridge Graduate Fellow from the University of Tennessee under appointment from Oak Ridge Associated Universities.

§Permanent address: Tennessee Technological University, Cookeville, Tennessee.

[1]M. T. McEllistrem, K. W. Jones, and D. M. Sheppard, Bull. Am. Phys. Soc. 13, 1426 (1968); C. Robertson, K. C. Chung, A. Mittler, K. Swartz, J. D. Brandenberger, and M. T. McEllistrem, Bull. Am. Phys. Soc. 14, 603 (1969).

[2]B. J. O'Brien, W. E. Dorenbusch, T. A. Belote, and J. Rapaport, Nucl. Phys. A104, 609 (1967).

[3]B. Cujec and I. M. Szöghy, Phys. Rev. 179, 1060 (1969).

[4]G. Brown, S. E. Warren, and R. Middleton, Nucl. Phys. 77, 365 (1966).

[5]A. Trier, J. Rapaport, T. A. Belote, and W. E. Dorenbusch, Nucl. Phys. A134, 396 (1969).

[6]S. Gorodetzky, C. Gehringer, P. Chevallier, R. Drouin, R. Manquenouille, and G. Sutter, J. Phys. (Paris) 29, 144 (1968).

[7]S. A. Hjorth, Arkiv Fysik 33, 147 (1966).

[8]M. G. Betigeri, H. H. Duhm, R. Santo, R. Stock, and R. Bock, Nucl. Phys. A100, 416 (1967).

[9]L. Birnstein, M. Harchol, A. A. Jaffe, and A. Tsukrovitz, Nucl. Phys. 84, 81 (1966).

[10]L. Birnstein, C. Drory, A. A. Jaffe, and Y. Zioni, Nucl. Phys. A97, 203 (1967).

[11]R. R. Johnson and G. D. Jones, Nucl. Phys. A122, 657 (1968).

[12]J. Vervier and H. H. Bolotin, to be published.

[13]E. Finckh, U. Jahnke, P. Pietrzyk, B. Schreiber, and A. Weidinger, to be published.

[14]C. Maples, G. W. Goth, and J. Cerny, Nucl. Data A2, 429 (1966); S. Raman, Nucl. Data B3 (No. 3, 4), 145 (1970). F. Everling, L. A. Koenig, J. Mattauch, and A. H. Wapstra, *Nuclear Data Tables*, compiled by K. Way *et al.* (Printing and Publishing Office, National Academy of Sciences – National Research Council, Washington, D. C.).

[15]C. H. Johnson, private communication.

[16]C. A. Baker, C. J. Batty, and I. E. Williams, Nucl. Instr. Methods 59, 125 (1968).

[17]P. O. Persson and S. E. Arnel, Arkiv Fysik 33, 371 (1967).

[18]N. Bouchard and B. Cujec, Nucl. Phys. A108, 529 (1968).

PHYSICAL REVIEW C VOLUME 2, NUMBER 1 JULY 1970

40-MeV Proton Inelastic Scattering on ^{50}Ti, ^{51}V, and ^{52}Cr and Its Microscopic Description*

B. M. Preedom,† C. R. Gruhn, T. Y. T. Kuo, and C. J. Maggiore

Department of Physics, Michigan State University, East Lansing, Michigan 48823

(Received 16 January 1970)

Proton inelastic scattering from ^{50}Ti, ^{51}V, and ^{52}Cr has been measured at 40 MeV. Angular distributions have been obtained from 10 to 80° for states up to 8 MeV of excitation in ^{50}Ti and ^{52}Cr, and to 4.5 MeV in ^{51}V. The cross sections for exciting the low-lying states that have relatively simple wave functions were analyzed in terms of a microscopic model, using realistic nucleon-nucleon forces. Core polarization is shown to be important, and it is seen that a strength obtained from the bound-state matrix elements of Kuo and Brown is adequate to describe the observed scattering. A macroscopic collective-model analysis of the data is also presented.

INTRODUCTION

Proton inelastic scattering from $^{50}_{22}Ti_{28}$, $^{51}_{23}V_{28}$, and $^{52}_{24}Cr_{28}$ has been measured at 40 MeV. In an earlier experiment, Funsten, Roberson, and Rost[1] studied these same nuclei, using the (p,p') reaction at 17.5 MeV. As in their work, the present data are analyzed within the framework of the distorted-wave (DW) approximation. However, recent theoretical developments make it possible to push this analysis somewhat further than was possible at the time of the earlier work. The present analysis is aided by the excellent optical-model studies which have been performed at 40 MeV.[2] Just as important, at this energy the angular distributions are more structured than at lower energies, and thus comparison of the results of theoretical calculations with the data should lead to less ambiguous conclusions.

Theoretical calculations based on three different models are presented. One of these models is the standard macroscopic collective model. Another is the empirical microscopic model.[3] In this model, it is assumed that the target nuclei can be described by simple shell-model wave functions, and the projectile-target interaction is fixed empiri-

cally. In particular, it is assumed that the low-lying states of ^{50}Ti, ^{51}V, and ^{52}Cr are described by the allowed couplings of $n(=2,3,4)$ protons in the $(f_{7/2})^n$ configuration. Using this assumption, the low-lying spectrum of these nuclei has been reasonably well reproduced in shell-model calculations using empirical interactions.[4] The data of Ref. 1 were analyzed using these two models.

A third model is the microscopic model with realistic forces. Recent work[5-7] has shown that interactions which relate directly to the free two-nucleon force can be used in nucleon-nucleus scattering calculations, provided the effects of long-range correlations in the target nuclei are explicitly taken into account. In this work, a pseudopotential based on the impulse approximation,[8,9] and the long-range part of the Kallio-Kolltveit interaction[10] are used for the projectile-target interaction. Exchange effects[11] are treated approximately.[5,7,13]

In ^{50}Ti, ^{51}V, and ^{52}Cr, long-range correlations appear as core polarization. These are effects due to the interaction of the valence nucleons with the core. Love and Satchler[12] have prescribed a method for including such effects which treats the core using the macroscopic collective model. In this procedure, one parameter characterizes the core for each multipole and valence configuration. This parameter can be determined directly from the effective charge for a corresponding γ transition [12] or from the bound-state matrix elements of Kuo and Brown.[5,7] The latter method is used in this work. Since the microscopic model with realistic forces contains no parameter determined from the present study, the comparison of the calculations based on this model with experiment should provide a direct test of the theoretical ideas involved.

EXPERIMENT

The data were obtained using 39.9-MeV protons from the Michigan State University sector-focused cyclotron. The beam was energy-analyzed using two 45° bending magnets with entrance and exit slits set to pass beam with an energy spread of 0.05%. The amount of beam on the target was monitored both by using a Faraday cup with an Elcor current integrator and a NaI(Tl) scintillation counter placed at 37.5° with respect to the beam. The targets were rolled, self-supporting foils of enriched ^{50}Ti and ^{52}Cr and natural ^{51}V. The subsequent uncertainty associated with the absolute cross sections was taken to be 15%.

The scattered protons were detected using a Ge(Li) solid-state detector in a surface-barrier configuration. Information concerning the fabrication, packaging, and use of this device has been published.[14] The vessel containing the Dewar and the crystal was mounted on a movable arm inside a 36-in. scattering chamber. The detector subtended a solid angle of 4.64×10^{-4} sr, and its angle relative to the beam could be determined to within 0.25°. Data were taken from 10 to 80° in 5° steps.

Spectra of protons scattered from ^{50}Ti, ^{51}V, and ^{52}Cr at a lab angle of 30° are shown in Fig. 1. The abscissa has been calibrated in terms of excitation energy above the ground state to be able to compare relative positions of the observed states. The energy resolution of the peaks is ~40 keV full width at half maximum. The major contributions to this energy spread arise from the beam energy spread (~20 keV), the energy spread due to straggling losses in the detector package window (~20 keV), and the kinematic broadening (~10 keV at 30°) since the detector subtended an angle of 0.7°. The broad hump seen in the spectra at excitation energies above 10 MeV arises from the particular slit geometry used in the Ge(Li) package. This slit system was made up of a thick slit necessary to stop the 40-MeV protons, and a thin slit with a smaller aperture which removed the slit scattering from the thick slit by degrading the energy of such events. The thickness of the degrader slit was chosen such that protons passing through it would fall in the spectrum at those excitation energies where the (p,d) reaction contributes as background.

THEORY

The analysis presented here was done in the framework of the DW theory.[15] All DW calculations were made using the FORTRAN-IV version of the code JULIE.[16] The differential cross section is obtained from a transition amplitude, t_{fi}, between the initial and final states.

$$\frac{d\sigma}{d\Omega}=\frac{\mu_a\mu_b}{(2\pi\hbar^2)^2}\frac{k_b}{k_a}[(2J_A+1)(2S_a+1)]^{-1}\sum_{\substack{M_A M_B\\ m_a m_b}}|t_{fi}|^2,$$

where μ_a and μ_b are the reduced masses in the entrance and exit channels, respectively, k_a and k_b are the wave numbers, J_A is the target spin, and S_a is the spin of the incident projectile. The transition amplitude, using a zero-range approximation, is calculated from an integral of the form

$$t_{fi}\propto\int d\vec{r}\,\chi_f^{(-)*}(\vec{k}_f,\vec{r})\,G_{lsj}(\vec{r})\,\chi_i^{(+)}(\vec{k}_i,\vec{r}),$$

where χ_i and χ_f are the elastic scattering wave functions in the entrance and exit channels, respectively. The term $G_{lsj}(r)$ is referred to as the radial form factor. It is calculated from the matrix element $\langle f|V|i\rangle$, where V is the interaction re-

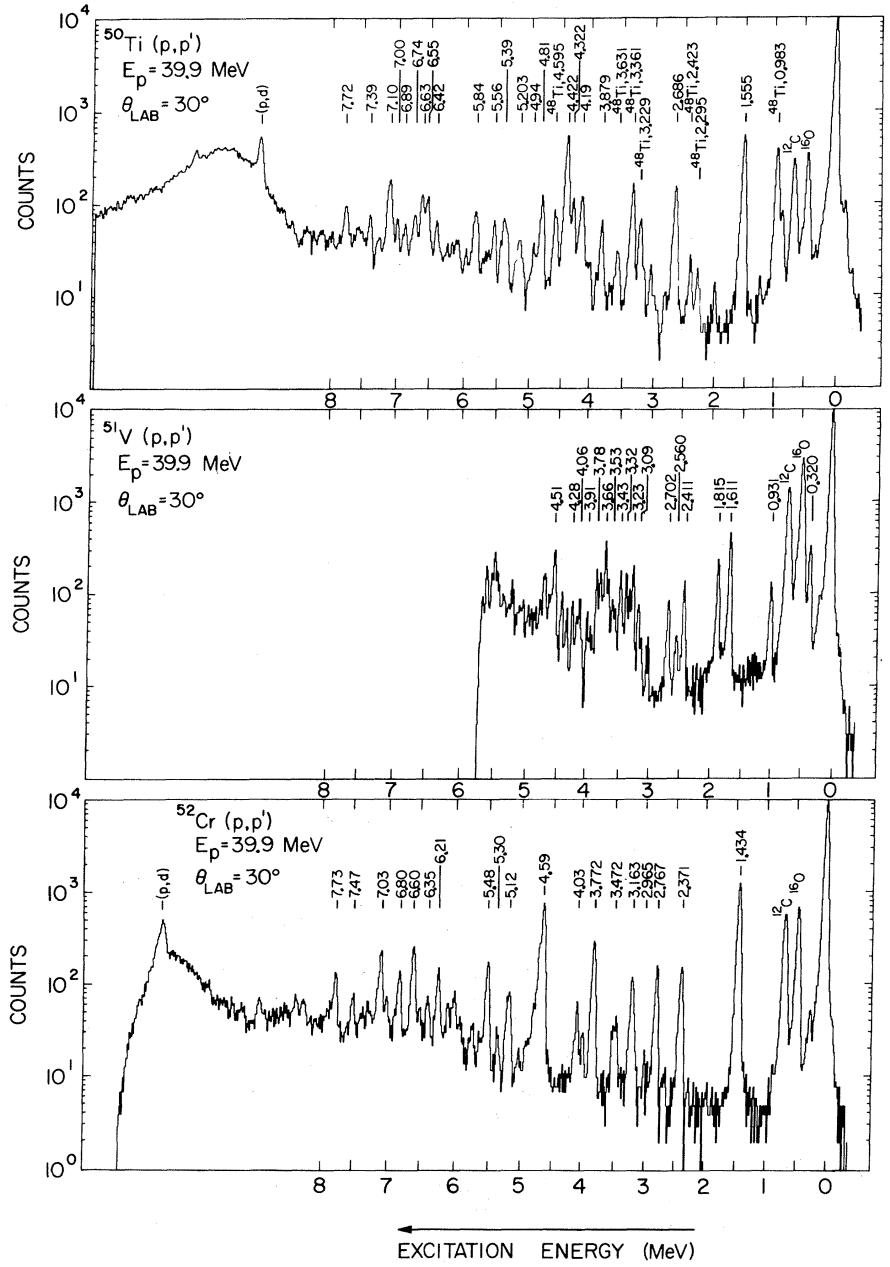

FIG. 1. Experimental spectra.

sponsible for the inelastic scattering. It is this factor that is subject to the model used to describe the nuclear states and the interaction.

A. Collective Model

The collective model of nuclear excitations is based on the deviations of the average nuclear field from spherical symmetry. These deviations are described by the theory of Bohr and Mottelson.[17] Because of the short-range nature of the nuclear force (small compared with nuclear radii), the deviations (deformations) modify the average nuclear field on a "macroscopic" scale. These "macroscopic" deviations are described in a "microscopic" manner by constructing the self-consistent fields acting on the particles and holes participating in the excitation. This connection between the "macroscopic" and "microscopic" description is made, for example, in the Hartree-Fock calculations of finite nuclear matter.[18]

The Hamiltonian describing the multipole deformation $\delta_L = \beta_L R_0$ in the "macroscopic" picture is given by[19]

$$H_L = \sum_M (-)^M \tfrac{1}{2} (B_L \dot{\alpha}_{LM} \dot{\alpha}_{L,-M} + C_L \alpha_{LM} \alpha_{L,-M}),$$

where

$$\beta_L = \sum_M |\alpha_{LM}|^2 ,$$

and B_L is the "mass transport" parameter and C_L is the "force constant" of the vibrator. These parameters are either calculated by more specific models or are determined by experiment.

As an example, in the classical incompressible irrotational hydrodynamical model, $(B_L)_{\rm hyd}$ is given by[19]

$$(B_L)_{\rm hyd} = \frac{(2L+1)}{L} \frac{AM\langle r^{2L-2}\rangle}{4\pi R_0^{2L-4}} ,$$

where AM is the mass of the nucleus. The quantity $\langle r^{2L-2}\rangle$ is evaluated using a uniform transition density with a radius determined by comparison with the equivalent Fermi distribution.[19,20] The excitation energy of such a vibrational state is given by

$$E_L = \hbar\omega_L = \hbar(C_L/B_L)^{1/2} .$$

The collective model for describing inelastic scattering[21] assumes the nuclear potential, as viewed by the projectile, undergoes a shape oscillation about a spherically symmetric potential. The form factor of such an oscillation is given by (for no spin transfer)

$$G_{L0L}(r) = -i^L(2L+1)^{-1/2}\beta_L R dU/dr , \qquad (1)$$

where

$$\beta_L^2 = \tfrac{1}{2}(2L+1)\hbar/(C_L B_L)^{1/2} ,$$

and the R are the real and imaginary radii for the real and imaginary parts of G_{L0L}, respectively. U is the empirically determined optical potential, excluding only the spin-orbit term. For quadrupole and octupole transitions, a term in $1/r^{L+1}$ was added coherently to take into account Coulomb excitation.[21]

The multipole fractional deformation, β_L, is extracted from the normalization of the calculated integrated cross section to the data. From this value, the deformation for the real part of the interaction is $\delta_L = \beta_L R_0$. Thus, knowing the excitation energy E_L and the deformation parameter δ_L, the "force constant" C_L and "mass transport" parameter B_L are found by

$$C_L = \tfrac{1}{2}(2L+1)(R_0^2/\delta_L^2)E_L , \qquad (2)$$

and

$$(B_L/\hbar^2) = \tfrac{1}{2}(2L+1)(R_0^2/\delta_L^2)(1/E_L) . \qquad (3)$$

The reduced transition probability, $B(EL;0\to L)$, is given[19,22] in terms of the deformation parameter δ_L by

$$B(EL;0\to L) = \left\{\frac{Ze(2L+1)}{4\pi R_0^{L-2}}\langle r^{2L-2}\rangle\right\}^2 \frac{\delta_L^2}{R_0^2} . \qquad (4)$$

We compare the results with the usual single-particle estimate (Weisskopf units)

$$B_{\rm sp}(EL;0\to L) = [(2L+1)/4\pi]e^2\langle r^L\rangle^2 ,$$

where $\langle r^L\rangle^2$ is calculated using a uniform charge distribution.

The value $G_{\rm sp}$ of the ratio $B(EL;0\to L)/B_{\rm sp}(EL;0\to L)$ measures in some sense the "collective strength" of the state. Along the same vein, it is of general interest to compare the reduced transition probabilities with two sum rules. The first is the non-energy-weighted sum rule, NEWSR[19] based on the shell model.

$$\text{NEWSR} = \sum_n B_n(EL;0\to L) = (e^2Z/4\pi)\langle r^{2L}\rangle , \qquad (5)$$

where the sum is over all states with spin L. The second sum rule is an energy-weighted sum rule,[23]

$$\text{EWSR} = \sum_n (E_n - E_0)B(EL;L\to 0)$$
$$= \frac{Z^2e^2L\hbar^2}{8\pi AM}(2L+1)^2\langle r^{2L+2}\rangle . \qquad (6)$$

This sum rule is model independent inasmuch as the nuclear Hamiltonian does not contain velocity-dependent potentials.

B. Microscopic Model

This model for inelastic scattering attempts to treat the nucleon-nucleus interaction as a sum of the basic nucleon-nucleon interactions. The formalism has been developed by Satchler.[3]

1. *Empirical Interactions*

If the total interaction is assumed to be a sum of scalar, single-particle operators which only act over a few active nucleons outside of an inert core, then the form factor, after summing over possible isospin transfer and assuming no spin transfer, can be written as

$$G_{L0L} = -\sqrt{2}\,4\pi V_{pp}^{s=0} M_L I_L(r) ; \qquad (7)$$

where $\sqrt{2} = (2s_a+1)^{1/2}$ and $s_a = \frac{1}{2}$ = spin of the incident proton; $V_{pp}^{s=0}$ is the strength of the "no spin-flip" interaction between the incident proton and protons in the target nucleus $[V_{pp}^{s=0} = V_N(a_{00}+a_{10})]$ in the notation of Ref. 3; M_L is a matrix element determined

TABLE I. Square of angular momentum matrix elements (M_L^2).

Transition	J_f^π	$L=2$	$L=4$	$L=6$
$(1f_{7/2})^2{}_{0^+} \rightarrow (1f_{7/2})^2{}_{J_f}$	2^+	0.0758	•••	•••
	4^+	•••	0.0372	•••
	6^+	•••	•••	0.0185
$(1f_{7/2})^3{}_{7/2^-} \rightarrow (1f_{7/2})^3{}_{J_f}$	$3/2^-$	0.065	0.117	•••
	$5/2^-$	0.185	0.009	0.024
	$9/2^-$	0.0313	0.0966	0.0184
	$11/2^-$	0.0842	0.0293	0.039
	$15/2^-$	•••	0.0338	0.0573
$(1f_{7/2})^3{}_{7/2^-} \rightarrow (1f_{7/2})^2{}_{0^+}(2p_{3/2})$	$3/2^-$	0.154	0.085	•••
$(1f_{7/2})^4{}_{0^+} \rightarrow (1f_{7/2})^4{}_{J_f}$; $v=2$	2^+	0.101	•••	•••
	4^+	•••	0.0495	•••
	6^+	•••	•••	0.0248

by the spins and the assumed configurations of the initial and final states of the nucleus and the transferred angular momentum (L); and $I_L(r)$ is an integral over the radial parts of the single-particle wave functions of the initial and final states, and the radial dependence assumed for the nucleon-nucleon interactions.

The angular momentum matrix elements have been evaluated for excitations within a $(1f_{7/2})^2$, $(1f_{7/2})^3$, and a $(1f_{7/2})^4$ configuration[1] and for excitations from a $(1f_{7/2})^3$ to a $(1f_{7/2})^2{}_{0^+}(2p_{3/2})$ configuration.[24] In this latter case, the state $(1f_{7/2})^2{}_{0^+}$ is considered to be the unique parent state. The values for the squares of the matrix elements are listed in Table I.

The single-particle radial wave functions were calculated both in an harmonic-oscillator well with a size parameter (α) equal to 0.498 F^{-1} and in a Woods-Saxon well. The DW calculations using these wave functions were not significantly different, so only the calculations using the Woods-Saxon eigenfunctions are presented below. The parameters of the Woods-Saxon well were those used for proton-pickup from ^{50}Ti, ^{51}V, and ^{52}Cr.[25] They are a radius of $1.20A^{1/3}$ F, a diffuseness of 0.65 F, a Coulomb interaction radius of $1.25A^{1/3}$ F, and a spin-orbit strength, in proton mass units, of $25\,V_0$. The total well depth, V_0, was determined by requiring that a $1f_{7/2}$ proton be bound by 8.06 MeV ($V_0 = 61.4$ MeV), and that a $2p_{3/2}$ proton be bound by 5.65 MeV ($V_0 = 64.7$ MeV). The choice of these energies is not critical. Angular distributions calculated using these $1f_{7/2}$ single-particle wave functions showed essentially no difference from those using $1f_{7/2}$ wave functions calculated for a binding energy of 12.2 MeV. Using Eq. (7), the strength $V_{pp}^{s=0}$ is derived from the normalization of the calculated cross sections to the experimentally observed values. That is, it is extracted in much the same way as one extracts deformation parameters in a collective model. For these calculations, a Yukawa radial dependence with a range parameter of 1 F^{-1} was chosen. Johnson, Owen, and Satchler[26] have shown for ^{90}Zr(p,p') that this is an acceptable value for the range. They also investigated the effects of using a Gaussian radial dependence, and found that it would not give the correct relative multipole dependence for L transfers from zero to eight.

2. *Realistic Interactions*

In order to include the effects of core polarization in the wave functions for the bound states of the target nuclei, terms containing excitations of the core have been added to the simple shell-model configurations. These additional terms explicitly introduce the fact that core nucleons participate in the transition and lead to the observed enhancements of transition rates over the single-particle estimates. According to Love and Satchler,[12] these effects can be included by modifying Eq. (7) such that

$$G_{L0L} = -\sqrt{2}\,4\pi M_L\left[V_{pp}^{s=0}\,I_L(r) - A_L R_0\,dU/dr\right],$$

where U is the usual optical potential which describes the elastic scattering from the target, R_0 is the nuclear radius (or interaction radius) in Fermis, and A_L is the single parameter which characterizes the effect of core polarization. In applying this relation, it is being assumed that the core participation is not introducing any appreciable configuration mixing into the valence states.

Love and Satchler fix the value of A_L by considering the γ transitions from each state. This method is limited to those states for which such measurements have been made. Petrovich and McManus have determined A_2, A_4, and A_6 for the $(1f_{7/2})^2$ configuration in ^{50}Ti from the G_{3p-1h} contributions to the bound-state matrix elements of Kuo

TABLE II. Interaction strengths ($V_{pp}^{S=0}$).

$$V_{pp}^{S=0}=V_R\frac{e^{-\alpha_R r}}{\alpha_R r}+V_I\frac{e^{-\alpha_I r}}{\alpha_I r}$$

	Impulse approx.		
	V_R=−22.8 MeV	V_I=−17.0 MeV	
	α_R=1.19 F^{-1}	α_I=1.32 F^{-1}	
	Eff IA		
	$V_I=\alpha_I=0$,	α_R=1 F^{-1}	
	V_R (L=2) (MeV)	V_R (L=4) (MeV)	V_R (L=6) (MeV)
^{50}Ti	−32.2	−35.6	−37.8
^{51}V	−32.2	−35.4	−37.9
^{52}Cr	−32.2	−35.6	−38.0

and Brown.[13] Since the bound-state matrix elements give a good fit to the spectrum, this method effectively uses the spectrum to determine the A_L. The values they have obtained are $A_2=0.159$, $A_4=0.110$, and $A_6=0.0775$. Since these numbers can be interpreted in terms of an effective charge for an $f\rightarrow f$ transition, it is assumed in this work that the same values of A_L are valid for excitations within the $(1f_{7/2})^3$ and the $(1f_{7/2})^4$ configurations.

Federman and Zamick[27] have recently calculated state-dependent effective charges for other transitions in this region. In particular, their calculations predict that the effective charge for transitions from an f to a p orbital differs by a factor of 0.15/0.21 from transitions within the f orbital. Therefore, the values of A_L for an $f\rightarrow p$ transition are taken to be just the $f\rightarrow f$ values modified by this factor.

The impulse approximation is valid for high-energy inelastic nucleon-nucleus scattering[9], and it has been shown to work at lower energies.[28] A problem occurs, however, in using this interaction in conjunction with the macroscopic vibrational model employed in the core polarization. The interaction is complex and its phase at the lower energies is incorrect, as is shown in calculations of the optical potential.[29] In order to circumvent this problem, DW calculations using a real, Yukawa interaction with a 1-F range were normalized to those calculations using the complete complex impulse-approximation interaction. This normalization determined a value for $V_{pp}^{S=0}$ which could be used in subsequent calculations. However, this method of obtaining an effective impulse-approximation interaction (Eff IA) now makes $V_{pp}^{S=0}$ dependent on the transferred angular momentum. The values for $V_{pp}^{S=0}$ for each nucleus are presented in Table II along with the complete complex 40-MeV impulse-approximation interaction from which they were derived.

The other interaction used, that due to Kallio and Kolltveit,[10] has a hard core and an exponential tail. It fits the s-wave phase shifts up to 300 MeV. The long-range part of this, obtained from the Scott-Moskowski separation method, represents the gross features of the Kuo-Brown reaction matrix.[30] Since this interaction represents only the direct term in the scattering, exchange effects must be explicitly included.[11] This was not necessary for the impulse approximation, since these effects are implicitly included in the pseudopotential. The exchange terms were included using a zero-range approximation of Petrovich *et al.*[7] This approximation has been checked against exact calculations of the exchange integrals, and has proven to be quite valid for the reactions presented here.[31]

ELASTIC SCATTERING

In order to obtain parameters for the distorted waves required in the calculations, the elastic scattering from each nucleus was analyzed. The optical potential used for the calculations had the form

$$U(r)=U_C-V_0f(x)+\left(\frac{\hbar}{m_\pi c}\right)^2V_{so}(\vec{\sigma}\cdot\vec{l})\frac{1}{r}\frac{d}{dr}f(x_{so})$$
$$-i\left(W-4W_D\frac{d}{dx'}\right)f(x'),$$

where

$$U_C=Z_Ae^2/r,\quad r\geq R_c$$
$$=(Z_Ae^2/2R_c)(3-r^2/R_c^2),\quad r\leq R_c,$$

$$R_c=1.25A^{1/3},$$

$$F(x)=(1+e^x)^{-1},$$

and

$$x=(r-r_0A^{1/3})/a.$$

The search code GIBELUMP[32] was used to vary the parameters in order to fit the observed elastic data. The criterion for a fit was the minimization of the quantity

$$\chi^2=\frac{1}{N}\sum_{i=1}^{N}\left[\frac{\sigma_{exp}(\theta_i)-\sigma_{th}(\theta_i)}{\Delta\sigma_{exp}(\theta_i)}\right]^2,$$

where N is the number of data points, $\sigma_{exp}(\theta_i)$ is the observed cross section at c.m. angle θ_i, and $\sigma_{th}(\theta_i)$ is the calculated cross section at θ_i. The relative uncertainty in the experimental cross section, $\Delta\sigma_{exp}(\theta_i)$, was taken to be 5% for all data points.

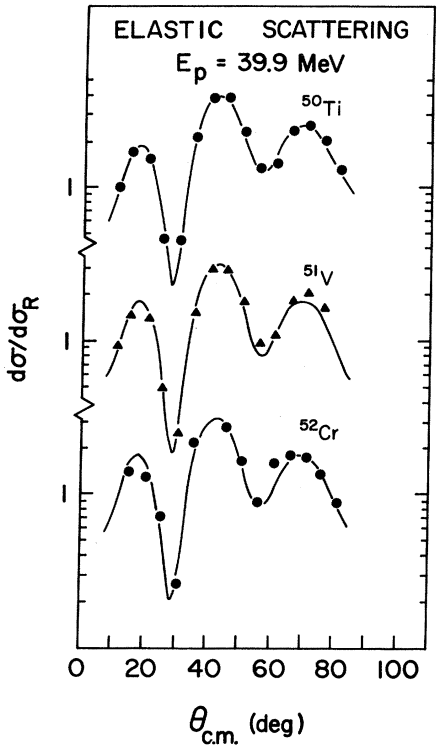

FIG. 2. Optical-model fits to elastic scattering data. The parameters are listed in Table III.

The parameters describing the elastic scattering from ^{50}Ti, ^{51}V, and ^{52}Cr use the average geometries (r_0 and a) and the average spin-orbit strength (V_{so}) found from elastic scattering and polarization measurements for 40-MeV protons on ten nuclei from ^{28}Si to ^{208}Pb.[2] The value of the imaginary surface strength (W_D) was taken to be the value found for ^{54}Fe. Using interpolated values as a starting point, the real well depth (V) and the imaginary volume depth (W) were varied by a small amount to obtain the fits to the elastic scattering data. The elastic scattering data, in ratio to Rutherford scattering, along with optical-model calculations are shown in Fig. 2. The parameters used in the optical-model calculations are listed in Table III. These parameters were used for all DW calculations presented in this study.

TABLE III. Optical parameters.

	V (MeV)	W (MeV)	χ^2
^{50}Ti	44.85	7.82	2.5
^{51}V	42.32	8.18	6.1
^{52}Cr	41.79	7.42	7.6

r_R=1.16 F, a_R=0.75 F, r_I=1.37 F,
a_I=0.63 F, r_{so}=1.064 F, a_{so}=0.738 F,
W_D=1.14 MeV, V_{so}=6.04 MeV.

EXPERIMENTAL ANALYSIS

A. ^{50}Ti

The states observed in ^{50}Ti are compared in Fig. 3 with the levels seen in (d,p),[33] (p,p'),[34] and in (α,α').[35] For levels whose identification is unambiguous, the energies are taken as those of Barnes *et al.*[33] All other levels are labeled with the energies determined from this work. The errors on

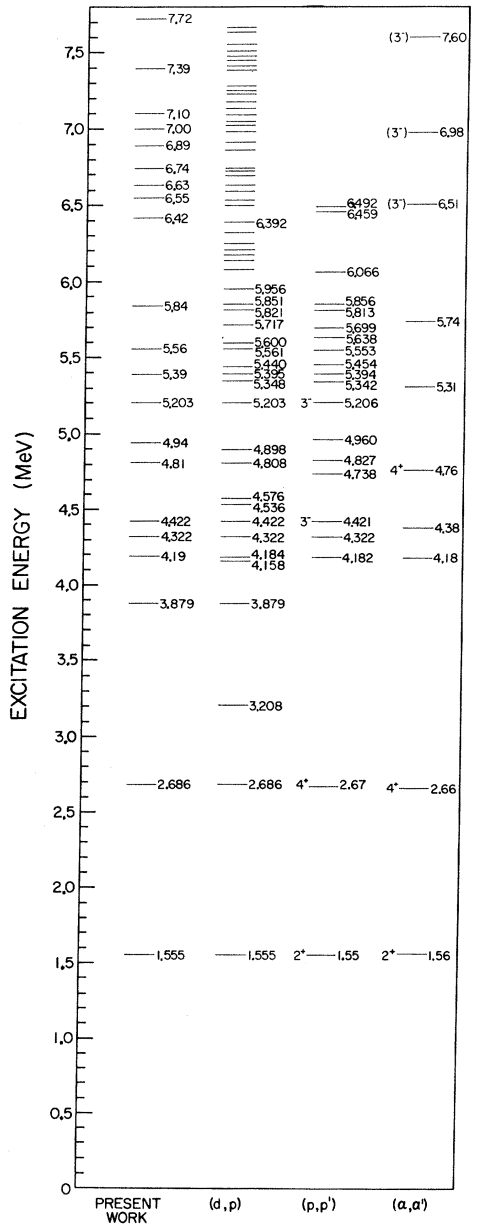

FIG. 3. Energy levels of ^{50}Ti. The levels are from Ref. 33 for (d,p), Ref. 34 for (p,p'), and Ref. 35 for (α,α').

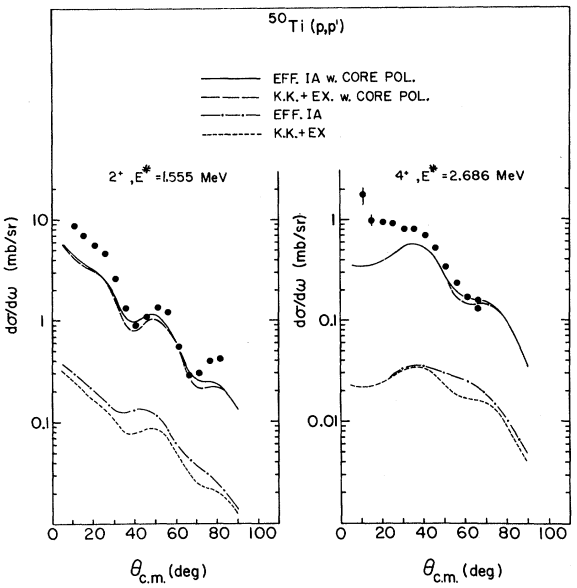

FIG. 4. A comparison of the experimental angular distributions for the first 2^+ and 4^+ states in ^{50}Ti, with microscopic calculations for excitations within a $(1f_{7/2})^2$ configuration.

these energies are approximately ±20 keV.

In Fig. 4 the angular distributions obtained for exciting the first 2^+ and 4^+ states are shown with various microscopic calculations assuming excitations within a $(1f_{7/2})^2$ configuration. The 6^+ state at 3.208 MeV, which is also attributed to this configuration, was not observed. These states appear to be good $(1f_{7/2})^2$ states from the reactions (n,d)[36] and $(d,^3\mathrm{He})$.[37] It is seen that without core polarization, both the impulse approximation and the Kallio-Kolltveit interaction plus exchange (K.K. + Ex) yield cross sections that are an order of magnitude too small. Also, although there is a difference between the predictions of the two interactions, it does not appear to be significant. In order to show a possible extreme, the calculations presented in Fig. 4 use harmonic-oscillator wave functions for the K.K. + Ex calculation, and Woods-Saxon wave functions for the Eff IA calculation. When the core polarization is included in the calculation, it is seen that the added strength brings the calculations into good agreement with the data, and makes the difference between the predictions of the two interactions even smaller. Because of this, only the impulse approximation will be used in the following calculations.

In Fig. 5, the microscopic calculations are compared with the shapes predicted by the collective model. The deformations obtained are also presented. The collective model does a good job in describing the over-all shape of the data. However, for the $L = 4$ transition, both calculations

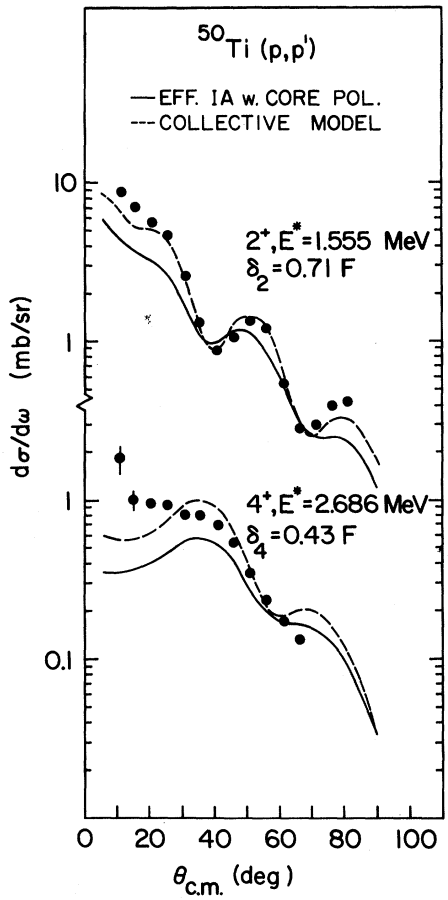

FIG. 5. Comparison of microscopic calculations and collective-model calculations with the experimental data.

miss the rise at small angles. It is interesting to note that this discrepancy has also been observed systematically in 40-MeV proton inelastic scattering from the Ni isotopes.[38] Although the collective model fits the data better, the microscopic-model calculations, which contain no free parameters, are still quite acceptable.

The data along with collective-model calculations are presented in Fig. 6 for the states which have undisputed spins and parities. It is seen that the data obtained here agree well with each assignment.

The data for all of the other states observed to be excited in ^{50}Ti are shown in Fig. 7. Again, collective-model calculations are compared with the measured distributions, and the extracted deformations are presented. The state at 3.879 MeV appears to be fairly well described by $L = 2$ transfer. The 4.19- and the 4.81-MeV levels are shown with the predictions for both an $L = 2$ and an $L = 4$ transfer. The present data favor the $L = 2$ assignment, but for the (α,α') reaction[35] the $L = 4$ description was used. The 4.19-MeV level is probably a dou-

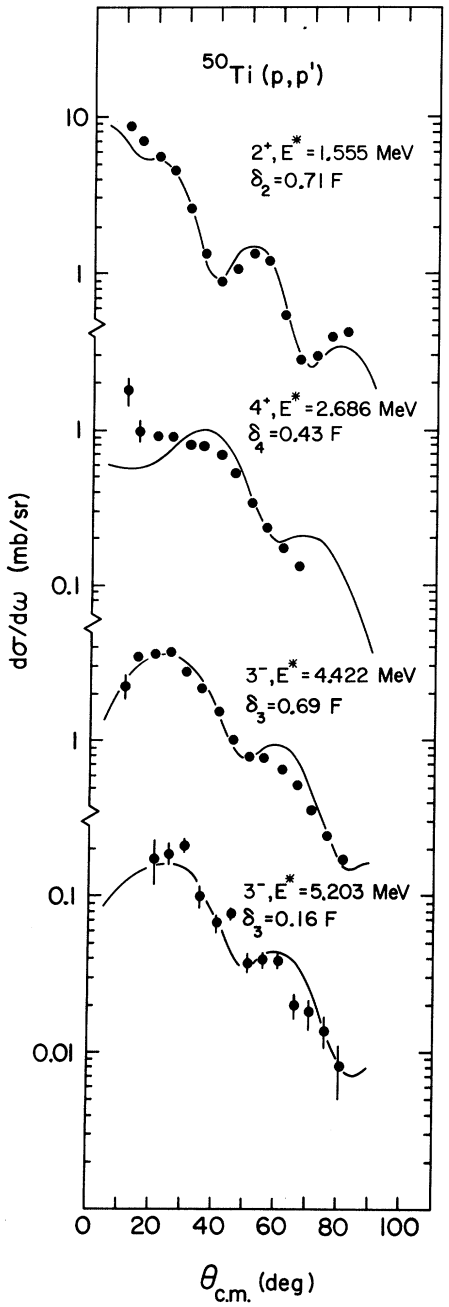

FIG. 6. Angular distributions for transitions to states of known spin and parity in ^{50}Ti. The curves are collective-model DW calculations.

blet made up of the levels seen at 4.184 and 4.158 MeV in the (d,p) reaction.[38] Because of the strong $L=1$ character of the distributions, they concluded that these levels were possibly made from the neutron configuration $(f_{7/2})^{-1}(p_{3/2})$. In a (t,p) reaction,[37] the 4.184-MeV state was seen with an $L=2$ transfer, and the 4.158-MeV state with an $L=4$ transfer. Thus the (p,p') reaction here seems to be exciting the 2^+ member more strongly than did the (α,α') reaction. The same situation might also exist for the 4.81-MeV level.

The states at 4.322 and at 4.94 MeV are well described by an $L=2$ transfer, while those at 5.39, 5.56, 5.84, 6.55, 6.63, 7.10, and 7.39 MeV are best described by an $L=3$ transfer. The $L=3$ transfer for the 7.10-MeV level is in agreement with the results of (α,α')[39] and (t,p)[40] reactions. The level at 7.72 MeV is shown with an $L=3$ calculation, allowing for the possibility that this level and a possible 3^- level observed in (α,α') at 7.60 MeV are the same levels. The experimental distributions obtained for the states at 6.42, 6.74, 6.89, and 7.00 MeV are also presented. For these states, no L transfer was found to give even qualitative agreement.

The values of δ_L for ^{50}Ti are listed in Table IV. These values of δ_L were used with Eq. (4) to find the reduced transition probabilities for the ground-state–to–excited-state transitions. In the approximation that the excitations are described in terms of harmonic vibrations, Eqs. (2) and (3) were used to calculate the "force constant," C_L, and "mass transport" parameters, B_L. The results of these calculations, along with a comparison of the reduced transition probability in single-particle units (G_{sp}), is given in Table V. The reduced transition probability to the first excited state is consistent with the electromagnetic results of Stelson and Grodzins,[41] as are also the values of B_L and C_L with the tabulated results of Wong.[42] In Table VI

TABLE IV. Deformations extracted for ^{50}Ti.

E^* (MeV)	J^π	L	δ_L (F)	$\pm\Delta$ (%)[a]
1.555	2^+	2	0.71	10
2.686	4^+	4	0.43	10
3.879		2	0.21	15
4.19		2	0.35	10
		4	0.39	20
4.322		2	0.29	10
4.422	3^-	3	0.69	10
4.81		2	0.29	15
		4	0.33	25
4.94		2	0.19	20
5.203	3^-	3	0.16	15
5.39		4	0.35	10
5.56		3	0.20	10
5.84		3	0.28	15
6.55		3	0.32	15
6.63		3	0.31	15
7.10		3	0.37	10
7.39		3	0.18	15
7.72		3	0.29	30

[a]The uncertainties are relative values obtained from the extreme credible fits of the DW calculations to the data.

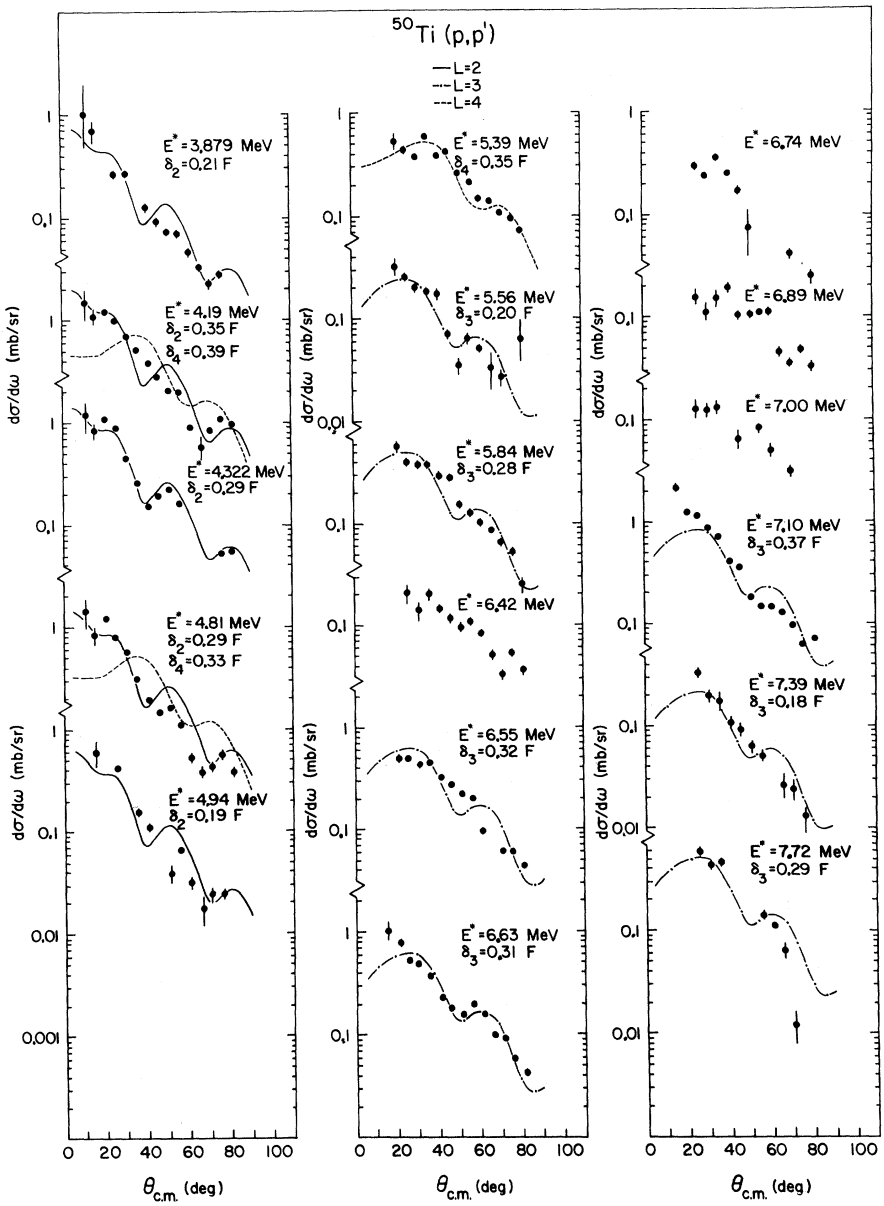

FIG. 7. Angular distributions for various states seen in ^{50}Ti(p,p'). The curves are collective-model DW calculations.

we list the fraction of the sum rule [Eqs. (5) and (6)] exhausted for each transition.

B. ^{51}V

The energy levels of ^{51}V observed in this work are presented in Fig. 8 along with a summary of levels seen below 5 MeV of excitation in (p,p') and (d,p) reactions.[43] Also shown are theoretical calculations predicting the levels of ^{51}V. Assuming an inert ^{48}Ca core, Auerbach[44] allows the three additional protons to be shared between the $1f_{7/2}$ and the $2p_{3/2}$ shells and Raj, Rustgi, and Singh[45] extend the basis to include the $1f_{5/2}$ and $2p_{1/2}$ shells. Using the coriolis coupling mode, Scholz and Malik[46] have also calculated the energy levels of ^{51}V as a function of possible permanent deformations. Their calculations, shown in Fig. 8, are those for a deformation of -0.32.

For the levels having unambiguous assignments, the excitation energies of Ref. 43 have been taken. A possible exception could be the 2.702-MeV state, since there is a close-lying state at 2.678 MeV. The identification of this level has been taken to be the $\frac{15}{2}^-$ state arising from the $(1f_{7/2})^3$ configuration, rather than the $\frac{3}{2}^+$ state which has a large amount of $1d_{3/2}$ hole strength.[47] This choice is supported by the (α,α') study of Peterson,[48] and it will also be seen that it leads to a consistent picture in the

TABLE V. Reduced transition probabilities, "mass-transport" parameters and "force constants" for ^{50}Ti. (The entries in columns 3, 5, and 6 are given in the form xy, where y is the power of 10 multiplying x.)

E_x^* (MeV)	L	$B(EL;\ 0\rightarrow L)$ (F^{2L})	G_{sp}	$B_L/\hbar^2$ (MeV)$^{-1}$	C_L (MeV)
1.555	2	0.431 3	5.5	0.687 2	0.166 3
2.686	4	0.735 5	2.7	0.195 3	0.141 4
3.879	2	0.377 2	0.5	0.315 3	0.474 4
4.322	2	0.720 2	0.9	0.148 3	0.277 4
4.422	3	0.878 4	5.9	0.358 2	0.700 3
4.940	2	0.309 2	0.4	0.302 3	0.737 4
5.203	3	0.472 3	0.3	0.566 3	0.153 5
5.390	4	0.487 5	1.8	0.147 3	0.427 4
5.560	3	0.738 3	0.5	0.339 3	0.105 5
5.840	3	0.145 4	1.0	0.165 3	0.562 4
6.550	3	0.189 4	1.3	0.112 3	0.482 4
6.630	3	0.177 4	1.2	0.118 3	0.520 4
7.100	3	0.252 4	1.7	0.776 2	0.391 4
7.390	3	0.597 3	0.4	0.315 3	0.172 5
7.720	3	0.155 4	1.0	0.116 3	0.692 4

description of the angular distributions observed in this work. The energies of the other levels in Fig. 8 have uncertainties of approximately ±20 keV.

The levels predicted by Auerbach include the $\frac{5}{2}^-$, $\frac{3}{2}^-$(0.86), $\frac{11}{2}^-$, $\frac{9}{2}^-$, and the $\frac{15}{2}^-$ states which are taken here to be excited through the $(1f_{7/2})^3$ configuration. The $\frac{3}{2}^-$(0.86) state, which could contain the $(1f_{7/2})^2{}_{0+}(2p_{3/2})$ single-particle excitation, is calculated by Auerbach to contain only about 1% of that configuration and a 25% admixture of a $(1f_{7/2})^2{}_{2+}$ $(2p_{3/2})$ state. Since this latter configuration would require a "two-step" process to excite it from the $(1f_{7/2})^3{}_{7/2-}$, $v=1$ ground state, this mode of excitation is not considered here. The description of this state is further supported by (^{3}He,d) reaction data[49] which indicate that it contains only about 1.5% of the $2p_{3/2}$ single-particle strength.

TABLE VI. Fraction of sum rules exhausted for ^{50}Ti.

E^* (MeV)	L	EWSR	NEWSR
1.555	2	0.045	0.172
2.686	4	0.016	0.055
3.879	2	0.010	0.015
4.322	2	0.021	0.029
4.422	3	0.086	0.149
4.940	2	0.010	0.012
5.203	3	0.005	0.008
5.390	4	0.021	0.036
5.560	3	0.009	0.013
5.840	3	0.019	0.025
6.550	3	0.027	0.032
6.630	3	0.026	0.030
7.100	3	0.040	0.043
7.390	3	0.010	0.010
7.720	3	0.027	0.026
Totals	2	0.086	0.228
	3	0.249	0.336
	4	0.037	0.091

A point should be made concerning two different models that have been used to describe the excitation of the low-lying states of ^{51}V. A "weak-coupling" model describes these states as resulting from a single $1f_{7/2}$ proton coupled to a ^{50}Ti(2^+) collective excitation. In this model, excitation of a state by inelastic scattering would have all of the characteristics of the excitation of the ^{50}Ti(2^+) state. A shell-model picture requires that only good parent states be taken into account. These two models have been compared to inelastic-scattering data,[1,24,48,50] and the "weak-coupling" model has been found to be inadequate to explain the data. This result is consistent with the work presented here.

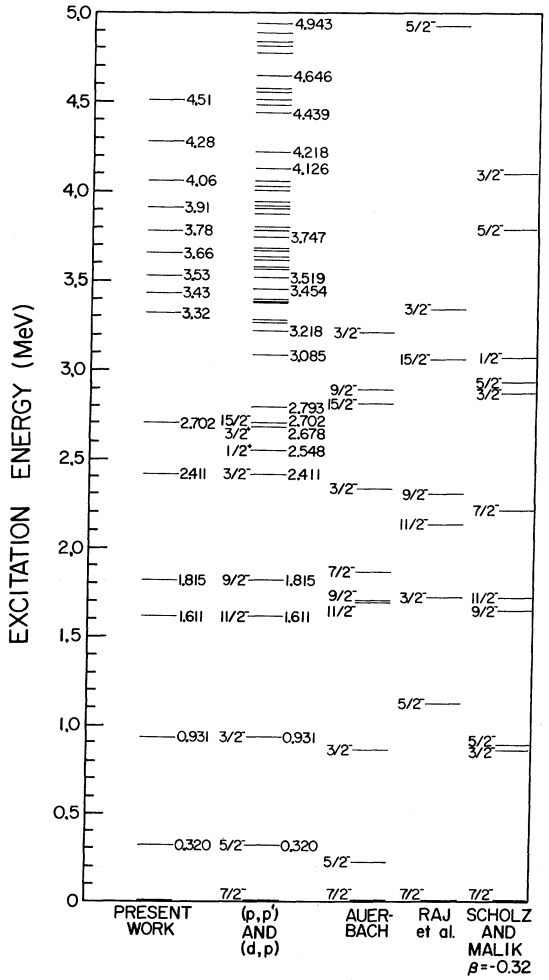

FIG. 8. Energy levels of ^{51}V. The levels for (p,p') and (d,p) are from Ref. 43. The calculations are by Auerbach (see Ref. 44), Raj *et al.* (see Ref. 45), and by Scholz and Malik (see Ref. 46).

Microscopic DW calculations are presented in Fig. 9 for angular momentum transfers of two, four, and six. The reduced cross sections (σ_L) have been normalized according to the equation in the figure. The angular momentum coupling coefficients (M_L^2) were given in Table I. The two interactions assumed for the calculations are the impulse approximation with the added core-polarization terms, and an interaction with a Yukawa radial form with a range of 1 F and a strength ($V_{pp}^{s=0}$) which was determined from an average normalization to the data. The core-polarization strength is the same as was used for the $(1f_{7/2})^2$ excitations in ^{50}Ti since this strength can be taken to represent, in some sense, the effective charge in a $1f_{7/2} \rightarrow 1f_{7/2}$ transition.

Combining the reduced cross sections for each of the possible $(1f_{7/2})^3$ states, one obtains the angular distributions shown in Fig. 10 along with the data. It is seen that the fits to the data are quite good, especially for the calculations employing the impulse approximation plus core polarization.

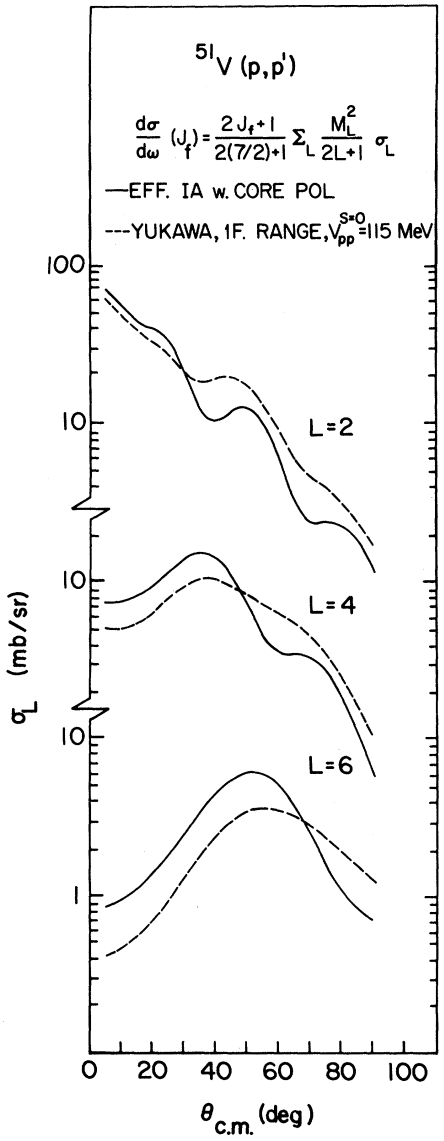

FIG. 9. Reduced cross sections for various multipole transitions. The calculations assume transitions within a $(1f_{7/2})^3$ configuration.

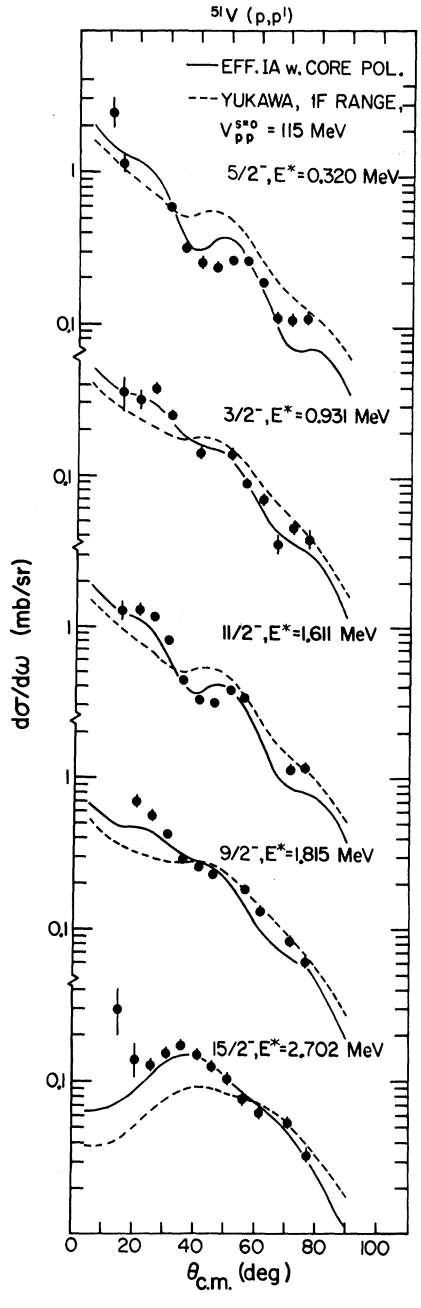

FIG. 10. Microscopic-model calculations compared with the data for transitions to states of the $(1f_{7/2})^3$ configuration.

Satchler[3] has indicated that a fair test of the microscopic model for inelastic scattering would be its ability to predict relative angular momentum transfers correctly. Since the three L transfers come into the above calculations in varying amounts for each state (e.g., $L=4$ dominates for the $\frac{5}{2}^-$ state, only $L=4$ and $L=6$ enter for the $\frac{15}{2}^-$ state), it appears that the microscopic model using the above interactions is indeed predicting the correct relative angular momentum transfers for 40-MeV inelastic proton scattering. At a lower proton energy (17.45 MeV) and with a Gaussian radial form for the interaction, Funsten, Roberson, and Rost[1] found some difficulty with the relative predictions. However, using the empirical shapes for the reduced cross sections derived from 17.5-MeV ^{52}Cr-(p,p') reactions to the 1.434-MeV (2^+), 2.371-MeV (4^+) and 2.767-MeV (4^+), and 3.114-MeV (6^+) states, Peterson[48] was able to correctly describe the magnitudes and general shapes of the observed angular distributions. For inelastic α scattering, Peterson[24] found that, in order to obtain agreement with the data, it was necessary to enhance the reduced cross section for an $L=2$ transfer by a factor of 4 while leaving unmodified the calculations for $L=4$ and 6.

Another transition in ^{51}V to a state whose configuration is considered to be known is that to the $\frac{3}{2}^-$ state at 2.411 MeV. This state contains a large amount of the $l=1$ single-particle strength in the ^{50}Ti(^{3}He,d) reaction,[47,49] and has been calculated[44] to have a large $(1f_{7/2})^2{}_{0^+}(2p_{3/2})$ strength. The microscopic DW calculations assuming a $(1f_{7/2})^3 \rightarrow (1f_{7/2})^2{}_{0^+}(2p_{3/2})$ transition are shown in Fig. 11 with the observed angular distribution. The core-polarization strength is that for a $1f \rightarrow 2p$ transition, as discussed earlier. Again the calculation using the impulse approximation plus core polarization reproduces both the magnitude and the shape of the experimental angular distribution rather well. It should also be noted that the calculation with only the Yukawa radial form fits the data, using the same strength as determined above. However, this might just be fortuitous, since the calculation then takes no account of the change in the core polarization even though this has been shown to be an important effect.

Auerbach predicts another $\frac{3}{2}^-$ level at 3.21 MeV that also has a large admixture of the $(1f_{7/2})^2{}_{0^+}(2p_{3/2})$ component. Such a state at 3.21 MeV has been observed with an $l=1$ distribution in the (^{3}He,d) reaction.[47,51] The states seen here at 3.32 and at

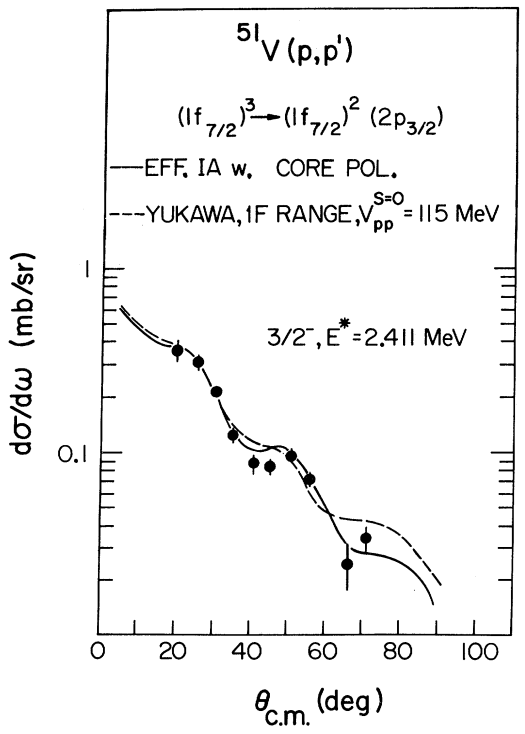

FIG. 11. Microscopic-model calculations compared with data for exciting the 2.411 MeV, $\frac{3}{2}^-$ state.

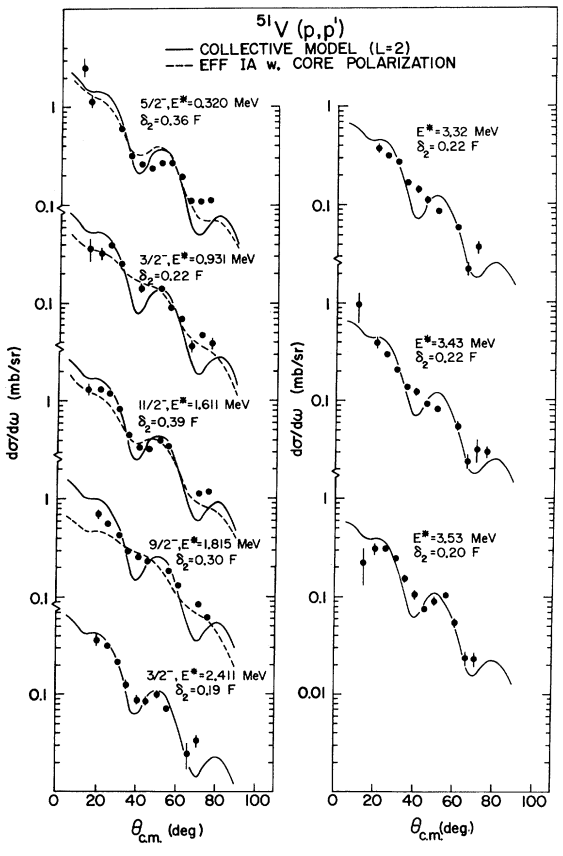

FIG. 12. Angular distributions of various transitions in ^{51}V.

3.43 MeV have distributions essentially the same in magnitude and shape as the 2.411-MeV state, and thus could be candidates for the predicted state.

Auerbach also predicts a $\frac{7}{2}^-$ state at 1.86 MeV which has remained unobserved. The calculations show this state to be essentially a pure $[(1f_{7/2})^2{}_{J_1} \times (2p_{3/2})]_{7/2^-}$ ($J_1 = 2, 4$) configuration, and thus it would require a "two-step" process to excite it.

In Fig. 12, the data for eight levels are compared with $L = 2$ collective-model DW calculations. For the $\frac{3}{2}^-$, $\frac{5}{2}^-$, $\frac{9}{2}^-$, and $\frac{11}{2}^-$ states, the microscopic calculations are also presented to show that these data favor the shell-model description over the "weak-coupling" model, as discussed earlier.

The data for the other analyzable states seen in this work are presented in Fig. 13. For the $\frac{15}{2}^-$ state, both an $L = 4$ collective-model DW calculation and a microscopic calculation are shown. It is seen that the collective model does not describe the experimental angular distribution very well. The states at 3.78 and at 4.51 MeV are shown with the predictions for an $L = 3$ transfer, and the state at 3.91 MeV with an $L = 2$ transfer. No collective-model calculation was found to adequately describe the states at 4.06 and at 4.28 MeV.

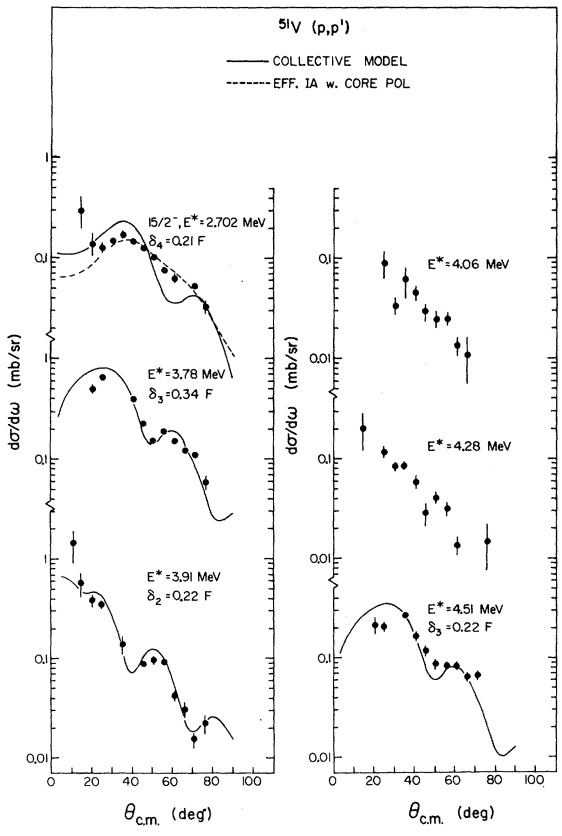

FIG. 13. Angular distributions of various transitions in ^{51}V.

TABLE VII. Deformations extracted for ^{51}V.

E^* (MeV)	J^π	L	δ_L (F)	$\pm\Delta$ (%)[a]
0.320	$5/2^-$	2	0.36	10
0.931	$3/2^-$	2	0.22	10
1.611	$11/2^-$	2	0.39	10
1.815	$9/2^-$	2	0.30	15
2.411	$3/2^-$	2	0.19	15
2.702	$15/2^-$	4	0.21	15
3.32		2	0.22	20
3.43		2	0.22	20
3.53		2	0.20	20
3.78		3	0.34	15
3.91		2	0.22	20
4.51		3	0.22	10

[a]The uncertainties are relative values obtained from the extreme credible fits of the DW calculations to the data.

In spite of the generally poor collective-model fits to the data, we list for completeness the deformations δ_L in Table VII. These values of δ_L were used to calculate the reduced transition probabilities along with the "mass-transport" and "force-constant" parameters. The results of these calculations are given in Table VIII. A comparison of the reduced transition probabilities to the first four excited states with other experiments is made in Table IX. It is seen that our results agree quite well with the results of (α,α')[24] and with 17.5 MeV (p,p'),[48] while there is disagreement with the results of the Coulomb excitation[52] for the $\frac{9}{2}^-$ excitation at 1.815 MeV. In Table X we present the fraction of the sum rule exhausted for each transition. It is interesting to note that in the first five transitions in ^{51}V we exhaust 3.5% of the 2^+ sum rule. This is to be compared with 4.5% for ^{50}Ti

TABLE VIII. Reduced transition probabilities, "mass-transport" parameters, and "force constants" for ^{51}V. (The entries in columns 3, 5, and 6 are given in the form xy, where y is the power of 10 multiplying x.)

E^* (MeV)	L	$B(EL;\ 0 \rightarrow L)$ (F^{2L})	G_{sp}	$B_L/\hbar^2$ $(\text{MeV})^{-1}$	C_L (MeV)
0.320	2	0.123 3	1.5	0.132 4	0.135 3
0.931	2	0.459 2	0.6	0.121 4	0.105 4
1.611	2	0.144 3	1.8	0.223 3	0.578 3
1.815	2	0.853 2	1.1	0.334 3	0.110 4
2.411	2	0.342 2	0.4	0.627 3	0.365 4
2.702	4	0.199 5	0.7	0.825 3	0.602 4
3.320	2	0.459 2	0.6	0.340 3	0.374 4
3.430	2	0.459 2	0.6	0.329 3	0.387 4
3.530	2	0.379 2	0.5	0.387 3	0.482 4
3.780	3	0.239 4	1.5	0.175 3	0.250 4
3.910	2	0.459 2	0.6	0.288 3	0.441 4
4.510	3	0.100 4	0.6	0.350 3	0.712 4

TABLE IX. Comparison of $B(E2;\ 0 \rightarrow L)$ (in F^4) for ^{51}V.

E^* (MeV)	J^π	Present results	(p,p')[a] (17.5 MeV)	(α,α')[b] (42 MeV)	Coul.[c] Ex.	Theory[d] ($\beta = -0.18$)
0.931	$3/2^-$	50	61	53	39	45
0.320	$5/2^-$	133	139	125	133	75
1.815	$9/2^-$	92	97	101	40	80
1.611	$11/2^-$	156	173	160	130	160

[a]Ref. 48. [b]Ref. 24. [c]Ref. 52. [d]Ref. 46.

and 5.1% for ^{52}Cr first 2^+ states. In the weak-coupling picture we would have expected these results to be comparable.

C. ^{52}Cr

The energy levels of ^{52}Cr seen in this work are compared in Fig. 14 with the level structure determined by (p,p') and (p,α) reactions,[53] and by (α,α'),[50] and by (e,e'),[54] along with various theoretical calculations. Where there is no ambiguity as to the identification of the level, the energies determined by Katsanos and Huizenga[53] are taken. The excitation energies of the other levels were determined in this work to be approximately ±20 keV. The calculations are those of McCullen, Bayman, and Zamick[4] (MBZ), assuming a pure $(1f_{7/2})^4$ configuration, of Auerbach,[44] allowing the $1f_{7/2}$ and $2p_{3/2}$ orbitals to mix, and those of Komoda,[55] which distributes the four protons among the $1f_{7/2}$, $2p_{3/2}$, $1f_{5/2}$, and $2p_{1/2}$ shells. The specific calculations of Komoda shown here use a Serber exchange mixture with a potential strength of 30 MeV and a range parameter equal to 1 F.

TABLE X. Fraction of sum rules exhausted for ^{51}V.

E^* (MeV)	L	EWSR	NEWSR
0.320	2	0.002	0.042
0.931	2	0.003	0.016
1.611	2	0.014	0.050
1.815	2	0.010	0.029
2.411	2	0.005	0.012
2.702	4	0.004	0.013
3.320	2	0.009	0.016
3.430	2	0.010	0.016
3.530	2	0.008	0.013
3.780	3	0.018	0.035
3.910	2	0.011	0.016
4.510	3	0.009	0.014
Totals	2	0.072	0.210
	3	0.027	0.049
	4	0.004	0.013

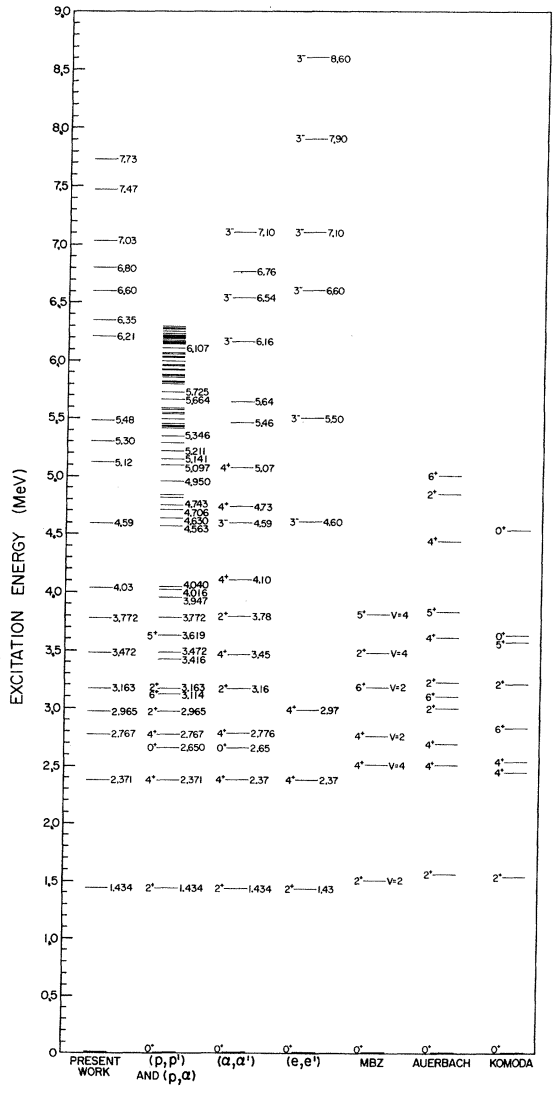

FIG. 14. Energy levels of ^{52}Cr. The levels for (p,p') and (p,α) are from Ref. 53, (α,α') from Ref. 50, and (e,e') from Ref. 44. The calculations are those of McCullen, Bayman, and Zamick (see Ref. 4), Auerbach (see Ref. 44), and Komoda (see Ref. 55).

In the MBZ calculations, seniority (v) is a good quantum number, since only effective three-body and four-body forces can cause seniority mixing in a pure configuration of identical particles.[56] However, once configuration mixing is allowed, then states of the same spin but different seniorities can mix. Thus the 2^+ states at 1.434 and 2.965 MeV and the 4^+ states at 2.371 and 2.767 MeV have seniority admixtures in the calculations of Komoda and of Auerbach.

The angular distributions to these states are shown in Fig. 15. Assuming a simple two-component wave function for the two states having the same spin, and also assuming that the interaction responsible for the excitation is a single-particle operator, then the ratio of the squares of the amplitudes is just given by the ratio of the experimental cross sections for exciting those states. Using the unit normalization condition, one then determines empirical values for the amplitudes.

In Table XI the ratios obtained here are compared with those calculated by Auerbach and by Komoda, and with similar quantities obtained from inelastic scattering,[1,50,54] transfer reactions,[57-59] and γ-decay branching ratio.[60] An immediate qualitative conclusion is that for the 2^+ states, seniority is a fairly good quantum number while for the 4^+ states, there is almost an equal admixture of $v=2$ and $v=4$ terms.

There is an interesting grouping of the values for the ratio of the 4^+ strengths apparent in Table XI. For the inelastic-scattering reactions, the first 4^+ state (4_1^+) is excited more strongly (i.e., has more $v=2$ strength) than the second 4^+ state. The transfer reactions and the γ decay show just the opposite. Also, the calculations of Auerbach agree with the latter values, while those presented for Komoda (with a range parameter equal to 1 F) agree with the values measured here. (It should be pointed out, however, that had another range parameter been taken in Komoda's calculation, the mixture could be inverted.) A possible explanation for this apparent discrepancy is that the transfer reactions may be sensitive to just the $(1f_{7/2})^4$, $v=2$ component of the wave function while the inelastic scattering can excite, in a coherent manner, all of the $v=2$ components in the wave function.

Since the interaction responsible for the excitations is taken to be a sum of single-particle operators, it follows that the DW calculation for a giv-

TABLE XI. Ratio of strengths of excitation for 2^+ and 4^+ states in ^{52}Cr.

Source	Reference	Ratio	$\frac{2_1^+(1.434)}{2_2^+(2.965)}$	$\frac{4_1^+(2.371)}{4_2^+(2.767)}$
(p,p')	present	$\left(\frac{\delta(J_1)}{\delta(J_2)}\right)^2$	59	1.20
(p,p')	1	$\left(\frac{\beta(J_1)}{\beta(J_2)}\right)^2$	2_2^+ not seen	1.66
(p,p')	48	$\left(\frac{\beta(J_1)}{\beta(J_2)}\right)^2$	21	1.64
(α,α')	48	$\left(\frac{\delta(J_1)}{\delta(J_2)}\right)^2$	2_2^+ not given	1.0
(α,α')	50	$\frac{\sigma_{\exp}(J_1, 17°)}{\sigma_{\exp}(J_2, 17°)}$	2_2^+ not seen	~1.0
(e,e')	54	$\frac{B(EL, J_1)}{B(EL, J_2)}$	2_2^+ not seen	1.3
$(^3\mathrm{He},d)$	57	$\frac{C^2S(J_1)}{C^2S(J_2)}$	2_2^+ not seen	0.62
(d,t)	59	$\frac{S(J_1)}{S(J_2)}$	2_2^+ not seen	0.83
(p,α)	58	$\frac{\sigma_{\exp}(J_1)}{\sigma_{\exp}(J_2)}$	1.27	0.76
γ decay	60	branching ratio	...	0.45
$f_{7/2}$-$p_{3/2}$ configuration	44	$\left\lvert\frac{f_{7/2}^4, v=2 \text{ in } J_1}{f_{7/2}^4, v=2 \text{ in } J_2}\right\rvert^2$	~100	0.60
$f_{3/2}$, $p_{3/2}$, $f_{5/2}$, and $p_{1/2}$ configuration	55	$\left\lvert\frac{f_{7/2}^4, v=2 \text{ in } J_1}{f_{7/2}^4, v=2 \text{ in } J_2}\right\rvert^2$	796	1.10

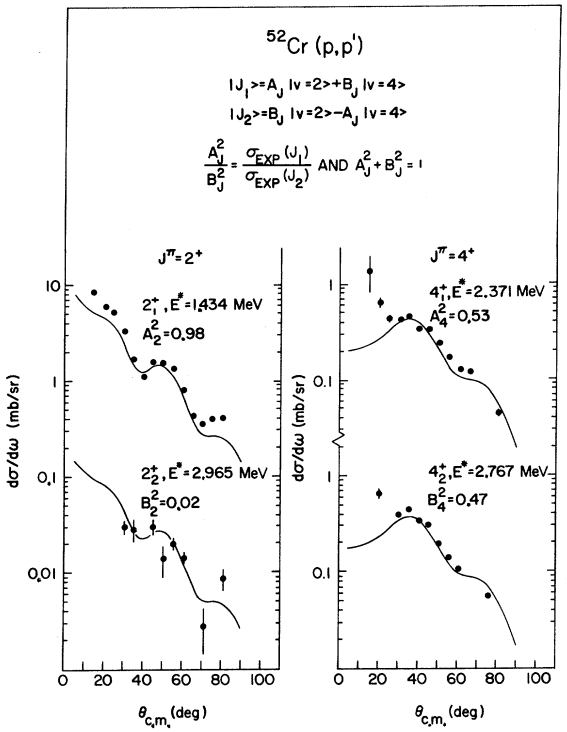

FIG. 15. Angular distributions for the excitation of states having a component of seniority (v) equal to two in their wave function. The calculations assume excitations within the $(1f_{7/2})^4$ configuration.

TABLE XII. Deformations extracted for ^{52}Cr.

E^* (MeV)	J^π	L	δ_L (F)	$\pm\Delta$ (%)[a]
1.434	2^+	2	0.77	10
2.371	4^+	4	0.34	10
2.767	4^+	4	0.31	10
2.965	2^+	2	0.10	20
3.163	2^+	2	0.28	10
3.472	4^+	4	0.13	15
3.772	2^+	2	0.40	10
4.03	4^+	4	0.19	10
4.59	3^-	3	0.65	15
5.12	4^+	4	0.20	15
5.30		3	0.19	15
5.48		4	0.35	10
6.21	3^-	3	0.29	10
6.35		4	0.16	10
6.60	3^-	3	0.32	10
6.80		2	0.25	10
7.03	3^-	3	0.34	15
7.73	3^-	3	0.25	15

[a]The uncertainties are relative values obtained from the extreme credible fits of the DW calculations to the data.

TABLE XIII. Reduced transition probabilities, "mass-transport" parameters, and "force constants" for ^{52}Cr. (The entries in columns 3, 5, and 6 are given in the form xy, where y is the power of 10 multiplying x.)

E^* (MeV)	L	$B(EL;\ 0\rightarrow L)$ (F^{2L})	G_{sp}	$B_L/\hbar^2$ $(\mathrm{MeV})^{-1}$	C_L (MeV)
1.434	2	0.620 3	7.5	0.650 2	0.134 3
2.371	4	0.591 5	1.9	0.363 3	0.204 4
2.767	4	0.491 5	1.6	0.374 3	0.287 4
2.965	2	0.105 2	0.1	0.186 4	0.164 5
3.163	2	0.820 2	1.0	0.223 3	0.223 4
3.472	4	0.864 4	0.3	0.170 4	0.204 5
3.772	2	0.167 3	2.0	0.916 2	0.130 4
4.030	4	0.185 5	0.6	0.684 3	0.111 5
4.590	3	0.977 4	6.0	0.399 2	0.841 3
5.120	4	0.205 5	0.7	0.486 3	0.127 5
5.300	3	0.835 3	0.5	0.405 3	0.114 5
6.210	3	0.194 4	1.2	0.148 3	0.572 4
6.350	4	0.131 5	0.4	0.612 3	0.247 5
6.600	3	0.237 4	1.5	0.115 3	0.499 4
6.800	2	0.653 2	0.8	0.130 3	0.602 4
7.030	3	0.267 4	1.7	0.953 2	0.471 4
7.730	3	0.145 4	0.9	0.160 3	0.957 4

en L transfer predicts the total strength for an excitation involving $\Delta v = 2$ [i.e., $\sigma_{DW}(L)\alpha|\langle J, v=2\,|\,V\,|\,0^+, v=0\rangle|^2$]. Assuming that $v=2$ excitations in the $(f_{7/2})^4$ configuration polarize the core in a manner similar to that of the $(f_{7/2})^2$ configuration in ^{50}Ti, one can then use the core-polarization strengths calculated for the ^{50}Ti excitations. Using the impulse approximation to obtain the interaction strengths, microscopic calculations similar to those presented earlier can be made for ^{52}Cr. These calculations, assuming just excitations within the $(f_{7/2})^4$ configuration, are compared with the data in Fig. 15. In order to determine the fraction of the total $v=2$ strength that each state should receive, one just multiplies the calculated strength by the amount of $v=2$ component in the wave function. It should be noted again that this coefficient is determined empirically, since it results from the ratio of the experimentally observed cross sections. Thus the first 2^+ state receives 98% of the calculated $L=2$, $v=2$ strength while the second 2^+

TABLE XIV. Comparison of ^{52}Cr(p,p') and ^{52}Cr(e,e'), $B(EL;\ 0\rightarrow L)$ (F^{2L}).

E^* (MeV)	L	(p,p') Present results	(e,e')[a]
1.434	2	620 ±120	742 ±58
2.371	4	59 100 ±12 000	97 200 ±16 840
4.59	3	9770 ±3000	9320 ±480

[a]See Ref. 54.

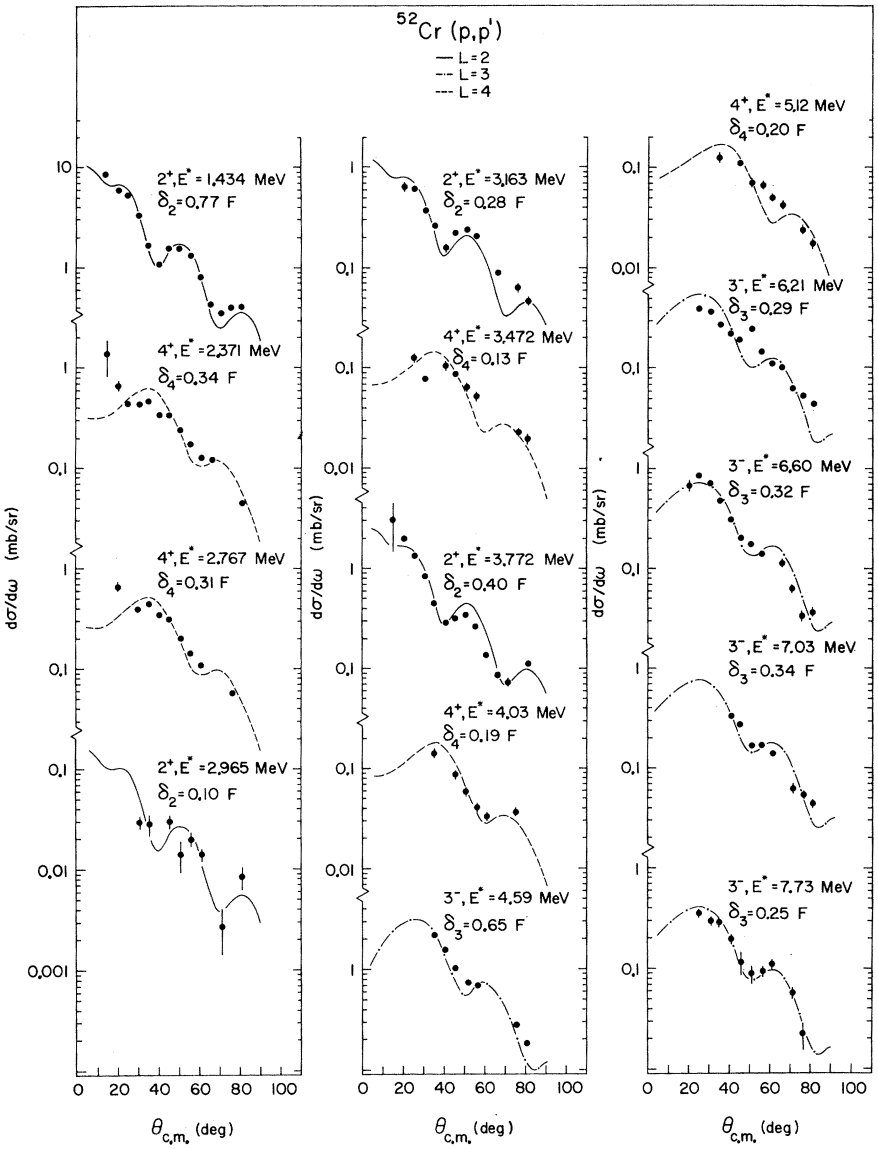

FIG. 16. Angular distributions for transitions to states of known spin and parity in ^{52}Cr. The curves are collective-model DW calculations.

receives only 2%. Similarly, the first 4^+ state receives 53% of the calculated $L=4$, $v=2$ strength and the second 4^+ gets 47%. It is seen from the excellent agreement in magnitude that the microscopic DW calculations are predicting the correct $v=2$ strengths for ^{52}Cr. As in previous sections, the shapes of the angular distributions are also well reproduced.

The data for various states of known spin and parity in ^{52}Cr are shown in Fig. 16 along with collective-model DW calculations and the extracted deformations. It is seen that these data are consistent with previous spin assignments.

In Fig. 17, data are presented for excitations leading to unidentified levels in ^{52}Cr. Collective-model calculations and extracted deformations are shown for the L values that best fit the angular distributions. For the 7.47-MeV state, no satisfactory calculation was found.

The values of δ_L for ^{52}Cr are presented in Table XII. The reduced transition probabilities along with the B_L, "mass-transport," and C_L, "force-constant," vibrational-model parameters are given in Table XIII. The values of B_L and C_L are approximately twice the values listed in the tables of Wong.[42] A portion of this discrepancy is accounted for by the fact that our reduced transition probability is low compared to the value used by Wong.

In Table XIV we compare the reduced transition probabilities for the lowest $L=2$, 3, and 4 transitions with the results obtained in the (e,e') reaction.[54] We find reasonable agreement for all three

transitions.

In Table XV we list the fraction of the sum rules exhausted for each transition. Comparing these results with those of $(\alpha, \alpha)^{61}$ using the EWSR, it is found that both reactions exhaust 5% of the EWSR in the first 2^+ state, and totals of 13 and 10%, respectively, of the EWSR for all observed 2^+ states.

For the lowest 3^- state, we obtain 8.3% of the sum rule versus the (α, α') result of 3%. And for

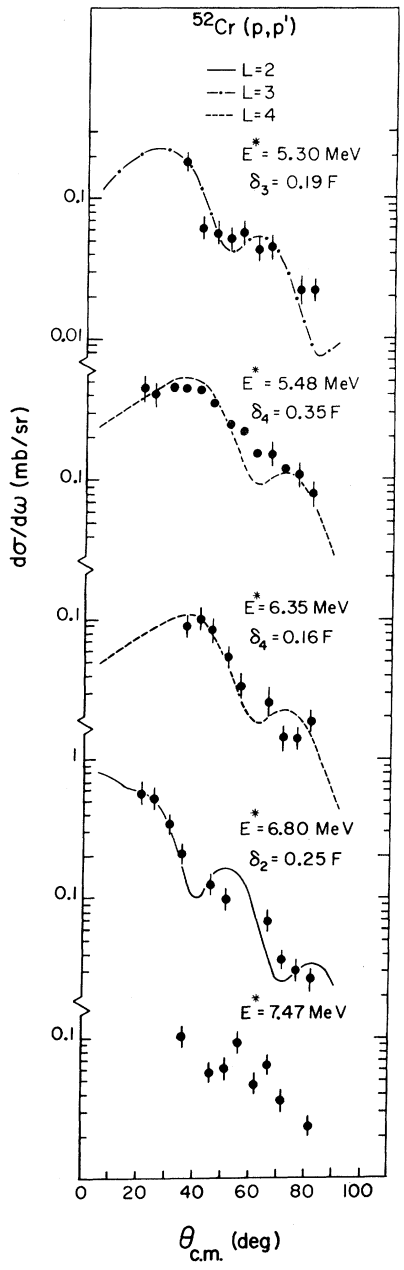

FIG. 17. Angular distributions to various states excited in ^{52}Cr(p,p'). The curves are collective-model DW calculations.

TABLE XV. Fraction of sum rules exhausted for ^{52}Cr.

E^* (MeV)	L	EWSR	NEWSR
1.434	2	0.051	0.215
2.371	4	0.009	0.037
2.767	4	0.009	0.030
2.965	2	0.002	0.004
3.163	2	0.015	0.028
3.472	4	0.002	0.005
3.772	2	0.036	0.058
4.030	4	0.005	0.011
4.590	3	0.083	0.141
5.120	4	0.007	0.013
5.300	3	0.008	0.012
6.210	3	0.022	0.028
6.350	4	0.005	0.008
6.600	3	0.029	0.034
6.800	2	0.025	0.023
7.030	3	0.035	0.039
7.730	3	0.021	0.021
Totals	2	0.129	0.328
	3	0.198	0.285
	4	0.037	0.104

all of the observed 3^- transitions, we obtain 20% versus the result of 8% obtained in (α, α'). In the (p,p') reaction for the first 4^+ state, we exhaust 1% versus 1.3% of EWSR obtained in (α, α').

SUMMARY AND CONCLUSIONS

From the analysis of the data presented here, it appears that the present form of the microscopic model of proton inelastic scattering gives an adequate description of the data. The angular distributions admittedly do not fit the data as well as those of a collective model, but on the other hand they do contain more specific information about the nuclear structure involved. This and the fact that the predicted magnitudes are not exactly correct indicate that there is still quite a bit of room for improvement. However, it is encouraging that one can make successful calculations using average optical potentials, a realistic nucleon-nucleon interaction, and realistic nuclear wave functions without any of the parameters being determined from the experiment under study.

We would like to express our gratitude to all of our colleagues at the Michigan State University Cyclotron Laboratory for their many invaluable discussions and comments, especially Professor H. McManus. Special thanks are given to Dr. F. Petrovich who proved to be an indispensible ally by his interest in the problem and by his patience in teaching us many of the subtleties of the calculations. We are also indebted to him for his constructive comments on the manuscript.

*Work supported in part by the National Science Foundation.

†Present address: Department of Physics, University of South Carolina, Columbia, South Carolina.

[1]H. O. Funsten, N. R. Roberson, and E. Rost, Phys. Rev. 134, B117 (1964).

[2]M. P. Fricke, E. E. Gross, B. J. Morton, and A. Zucker, Phys. Rev. 156, 1207 (1967).

[3]G. R. Satchler, Nucl. Phys. 77, 481 (1966).

[4]J. D. McCullen, B. F. Bayman, and L. Zamick, Phys. Rev. 134, B515 (1964).

[5]F. Petrovich, Ph. D. thesis, Michigan State University, 1970 (unpublished).

[6]D. Agassi and R. Schaeffer, Phys. Letters 26B, 703 (1968).

[7]F. Petrovich, H. McManus, V. A. Madsen, and J. Atkinson, Phys. Rev. Letters 22, 895 (1969).

[8]A. K. Kerman, H. McManus, and R. M. Thaler, Ann. Phys. (N.Y.) 8, 551 (1959).

[9]R. M. Haybron and H. McManus, Phys. Rev. 136, B1730 (1964); 136, B638 (1965).

[10]A. Kallio and K. Kolltveit, Nucl. Phys. 53, 87 (1964).

[11]K. A. Amos, V. A. Madsen, and I. E. McCarthy, Nucl. Phys. A94, 103 (1967).

[12]W. G. Love and G. R. Satchler, Nucl. Phys. A101, 424 (1967).

[13]F. Petrovich and H. McManus, to be published.

[14]C. R. Gruhn, T. Kuo, C. Maggiore, B. Preedom, L. Samuelson, and J. Chander, IEEE Trans. Nucl. Sci. 15, No. 3, 337 (1968).

[15]G. R. Satchler, Nucl. Phys. 55, 1 (1964).

[16]R. H. Bassel, R. M. Drisko, and G. R. Satchler, Oak Ridge National Laboratory Report No. ORNL-3240, 1962 (unpublished); and "Oak Ridge National Laboratory Memrandum to the Users of the Code JULIE," 1966 (unpublished).

[17]A. Bohr and B. Mottelson, Kgl. Danske Videnskab. Selskab Mat.-Fys. Medd. 27, No. 16 (1953).

[18]M. Baranger, in *Proceedings of the International Conference on Nuclear Physics, Gatlinburg, Tennessee, 12-17 September 1966,* edited by R. L. Becker and A. Zucker (Academic Press Inc., New York, 1967), p. 659; G. Ripka, in *Proceedings of the International Conference on Nuclear Physics, Gatlinburg, Tennessee, 12-17 September 1966,* edited by R. L. Becker and A. Zucker (Academic Press Inc., New York, 1967), p. 833; F. Villars, in *Nuclear Physics, Proceedings of the International School of Physics, "Enrico Fermi," Course XXIII,* edited by V. F. Weisskopf (Academic Press Inc., New York, 1963), p. 1; and J. Bar-Touv and C. A. Levinson, Phys. Rev. 153, 1099 (1967); D. R. Bes and R. A. Sorenson, Advances in Nucl. Phys. 2, 129 (1969).

[19]A. M. Lane and E. Pendelbury, Nucl. Phys. 15, 39 (1960).

[20]C. R. Gruhn, B. M. Preedom, and K. Thompson, Phys. Rev. Letters 23, 1175 (1969).

[21]R. H. Bassel, G. R. Satchler, R. M. Drisko, and E. Rost, Phys. Rev. 128, 2693 (1962).

[22]L. W. Owen and G. R. Satchler, Nucl. Phys. 51, 155 (1963).

[23]O. Nathan and S. G. Nilsson, in *Alpha-, Beta-, Gamma-Ray Spectroscopy,* edited by K. Siegbahn (North-Holland Publishing Company, Amsterdam, The Netherlands, 1965), Chap. X.

[24]R. J. Peterson, Phys. Rev. 172, 1098 (1968).

[25]E. Newman and J. C. Hiebert, Nucl. Phys. A110, 366 (1968).

[26]M. B. Johnson, L. W. Owen, and G. R. Satchler, Phys. Rev. 142, 748 (1966).

[27]P. Federman and L. Zamick, Phys. Rev. 177, 1534 (1969).

[28]F. Petrovich, D. Slanina, and H. McManus, Bull. Am. Phys. Soc. 12, 12 (1967).

[29]D. Slanina, Ph. D. thesis, Michigan State University, 1969 (unpublished).

[30]G. E. Brown, *Unified Theory of Nuclear Models* (North-Holland Publishing Company, Amsterdam, The Netherlands, 1965).

[31]F. Petrovich, private communication.

[32]Oak Ridge National Laboratory FORTRAN-IV computer code written by F. G. Perey and modified by R. M. Haybron (unpublished).

[33]P. D. Barnes, C. K. Bockelman, O. Hansen, and A. Sperduto, Phys. Rev. 140, B42 (1965).

[34]W. S. Gray, R. A. Kenefick, and J. J. Kraushaar, Nucl. Phys. 67, 565 (1965).

[35]J. L. Yntema and G. R. Satchler, Phys. Rev. 161, 1137 (1967).

[36]K. Ilakovac, L. G. Kuo, M. Petravíc, I. Šlaus, P. Tomaš, and G. R. Satchler, Phys. Rev. 128, 2739 (1962).

[37]F. Hinterberger, G. Mairle, U. Schmidt-Rohr, P. Turek, and G. Wagner, Z. Physik 202, 236 (1967).

[38]K. M. Thompson, Ph. D. thesis, Michigan State University, 1969 (unpublished); C. R. Gruhn, B. M. Preedom, and K. M. Thompson, to be published.

[39]A. M. Bernstein and E. P. Lippincott, Phys. Rev. Letters 17, 321 (1966).

[40]S. Hinds and R. Middleton, Nucl. Phys. A92, 422 (1967).

[41]P. H. Stelson and L. Grodzins, Nucl. Data A1, 21 (1965).

[42]C. Y. Wong, Nucl. Data A4, 271 (1968).

[43]M. E. deLópez, M. Mazari, T. A. Belote, W. E. Dorenbusch, and O. Hansen, Nucl. Phys. A94, 673 (1967).

[44]N. Auerbach, Phys. Letters 24B, 260 (1967).

[45]R. Raj, M. L. Rustgi, and R. P. Singh, Phys. Rev. 181, 1536 (1969).

[46]W. Scholz and F. B. Malik, Phys. Rev. 147, 836 (1966); Malik and Scholz, Phys. Rev. 150, 919 (1966).

[47]D. J. Pullen, B. Rosner, and O. Hansen, Phys. Rev. 177, 1568 (1969).

[48]R. J. Peterson, Ann. Phys. (N.Y.) 53, 40 (1969).

[49]B. J. O'Brien, W. E. Dorenbusch, T. A. Belote, and J. Rapaport, Nucl. Phys. A104, 609 (1967).

[50]J. R. Meriwether, I. Gabrielli, D. L. Hendrie, J. Mahoney, and B. G. Harvey, Phys. Rev. 146, 804 (1966).

[51]C. St. Pierre, P. N. Maheshwari, D. Doutriaux, and L. Lamarche, Nucl. Phys. A102, 433 (1967); B. Čujec and I. M. Szöghy, Phys. Rev. 179, 1060 (1969).

[52]O. F. Afonin, A. P. Grinberg, I. K. Lemberg, and I. N. Chugunov, Yadern. Fiz. 6, 219 (1967) [transl.: Soviet J. Nucl. Phys. 6, 160 (1968)].

[53]A. A. Katsanos and J. R. Huizenga, Phys. Rev. 159, 931 (1967).

[54]J. Bellicard, P. Barreau, and D. Blum, Nucl. Phys. 60, 319 (1964).

[55]T. Komoda, Nucl. Phys. 51, 234 (1964).

[56]C. Schwartz and A. de-Shalit, Phys. Rev. 94, 1257

(1954); I. Talmi, *ibid.* 126, 1096 (1962).
[57]D. D. Armstrong and A. G. Blair, Phys. Rev. 140, B1226 (1965).
[58]G. Brown, J. G. B. Haigh, and A. E. MacGregor, Nucl. Phys. A97, 353 (1967).
[59]W. Fitz, J. Heger, R. Jahr, and R. Santo, Z. Physik 202, 109 (1967).
[60]M. S. Freedman, F. Wagner, Jr., F. T. Porter, and H. H. Bolotin, Phys. Rev. 146, 791 (1966).
[61]A. Bernstein, in *Advances in Nuclear Physics,* edited by M. Baranger and E. Vogt (Plenum Press, Inc., New York, to be published), Vol. III.

PHYSICAL REVIEW C VOLUME 2, NUMBER 1 JULY 1970

Shell-Model Structure of $^{42-50}$Ca†

J. B. McGrory, B. H. Wildenthal, * and E. C. Halbert
Oak Ridge National Laboratory, Oak Ridge, Tennessee 37830
(Received 12 January 1970)

The low-lying states of the calcium isotopes ^{42}Ca through ^{50}Ca are discussed within the framework of the conventional shell model. An inert ^{40}Ca core is assumed. Calculations are made in several basis-vector spaces involving active $0f_{7/2}$, $1p_{3/2}$, $0f_{5/2}$, $1p_{1/2}$, and $0g_{9/2}$ neutron orbits. In one set of calculations, we use a "realistic" effective interaction derived for this mass region by Kuo and Brown. The shell-model results suggest that, in this effective interaction, the interactions of $f_{7/2}$ neutrons with $p_{3/2}$, $p_{1/2}$, and $f_{5/2}$ neutrons are too strong. In other calculations, with a modified Kuo-Brown interaction, we find the calculated spectra for the low-lying states of the calcium isotopes are in agreement with observed spectra, with several significant exceptions. The exceptions are that the second 0^+ and 2^+ states observed in ^{42}Ca, ^{44}Ca, and ^{46}Ca are not accounted for in the calculation. Calculated spectroscopic factors for $f_{7/2}$ transfers are in good agreement with experimental spectroscopic factors, and the observed centroids of the $p_{3/2}$ single-particle strengths are reasonably well reproduced. Our results also indicate that "core-excitation" effects are significant above about 2.5 MeV in ^{42}Ca through ^{48}Ca.

I. INTRODUCTION

The low-lying levels of the calcium isotopes have long been of interest to both experimental and theoretical physicists. Thirteen isotopes of calcium are known, six of which are stable. Using these six stable isotopes as targets, it is possible to study the level structure of all 13 isotopes with one- and two-nucleon pickup and stripping reactions. Thus it has been possible to accumulate a large amount of experimental information about these nuclei. The calcium isotopes comprise a convenient set of nuclei from a theoretical standpoint too. With the exception of the lightest two isotopes, ^{38}Ca and ^{39}Ca, it is useful to make the approximation that each calcium isotope has a doubly-magic $A=40$ core. In this approximation, all the active particles outside the $A=40$ core are neutrons. Then with some further simplifications (which we shall discuss), detailed shell-model treatments of the Ca isotopes become quite feasible. These further simplifications are suggested by the spectrum of single-particle states that seems to be appropriate for the calcium isotopes. The single-particle spectrum will be discussed in more detail in Sec. II.

Many calculations of the level structures of the calcium isotopes have been reported previously. It is useful to describe briefly several such calculations, as a background to the investigation reported here. In the earliest systematic calculations of the calcium isotopes,[1-3] only pure $f_{7/2}$-neutron configurations were included. The structure of the single-particle spectrum, as discussed below, suggests that this pure-$f_{7/2}$ model is a reasonable first-order approximation. In this approximation the effective Hamiltonian is completely specified by five parameters: the binding energy of the $f_{7/2}$ neutron to the ^{40}Ca core, and the four two-body matrix elements $\langle f_{7/2}^2 J| V| f_{7/2}^2 J\rangle$ with $J=0$, 2, 4, and 6. (Here, and throughout this paper, V represents the two-body part of the effective Hamiltonian.) In the calculations of Refs. 1–3, these five parameters were taken directly from the experimentally observed spectra of ^{41}Ca and ^{42}Ca. These calculations satisfactorily reproduced the observed energies and spins of many of the low-lying states of the calcium isotopes. The levels which are accounted for by this pure-$f_{7/2}$ model will be referred to as $f_{7/2}$ states.